EFFECT OF INFILTRATION OF PROCESS MEDIA ON THE THERMAL SHOCK RESISTANCE OF REFRACTORY MATERIALS (STRUCTURAL SPALLING)

Erwan Brochen, Christian Dannert,
Forschungsgemeinschaft Feuerfest e. V. at the European Centre for Refractories, Höhr-Grenzhausen, Germany

Florian Holleyn, Olaf Krause
Koblenz University of Applied Sciences, Höhr-Grenzhausen, Germany

ABSTRACT
The infiltration of liquid metal, slag or gases significantly changes the chemical and mineralogical composition of refractory materials, and thus alters their physical characteristics to such an extent that the thermomechanical properties of these infiltrated areas are no longer comparable with those of the non-infiltrated material. The transition between the infiltrated zone and the fresh material is particularly critical, as the thermomechanical properties change abruptly here. This promotes the formation of cracks in the transition zone or even the spalling of the infiltrated areas (structural spalling) during operational thermal cycling.
An application-oriented testing strategy has been developed to simulate and assess the impact of practice-relevant thermal shocks on the structural integrity of partly infiltrated refractory materials used as wear lining in the metallurgical industry. Test pieces made of refractory castables were infiltrated in a controlled manner and then exposed to high temperature thermal shocks while the decrease of the ultrasonic velocity inside the test piece was assessed in-situ and contactless after each thermal shock.
The level of damage of the test pieces increased after each thermal shock cycle, which correlated with the formation of macrocracks. Though significant damage can also be assessed on thermo-shocked non-infiltrated test pieces, infiltrated test pieces displayed far greater damaging features (doubled damage parameter values and larger macrocracks) both quantitatively (using damage parameter) and optically (macrocrack formation). Notably, cracks at the transition zone between infiltrated and fresh material can be observed.

INTRODUCTION
While the thermal shock resistance of refractory is being the subject of intensive research [1-2], especially in order to understand and prevent spalling, this focuses almost exclusively on fresh refractory materials that have not yet interacted with a process medium. In practice, especially for the most prominent refractory applications, infiltration by process media (liquid metal, slag or gases) is inevitable and significantly changes the chemical and mineralogical composition of refractory materials in the wear lining. This alters the physical characteristics of the infiltrated layer to such an extent that their thermomechanical properties are no longer comparable with those of the non-infiltrated material. The transition between the infiltration zone and the non-infiltrated material in the refractory lining is particularly critical, as the thermomechanical properties change abruptly here. This promotes the formation of cracks in the transition zone or even the spalling of the infiltrated areas (so-called structural spalling) during operational thermal cycling and/or when such a lining cools down.

DISTINCTION BETWEEN THERMAL SPALLING AND STRUCTURAL SPALLING
Spalling refers to the process by which thermomechanical stresses in a refractory material led to the formation of cracks and the subsequent breakage of large pieces of the material. However, the literature generally distinguishes between thermal spalling, which is purely thermomechanically induced, and structural spalling, which is triggered by a change in the material's properties due to the infiltration of process media into the refractory material [3]. In principle, both processes overlap in service and are difficult to separate from each other.
Thermal spalling is essentially the result of macroscopic thermal stresses developing in refractory components or linings. The primary reasons for this are as follows:
- hindrance of free thermal expansion due to design restrictions;
- stationary and/or transient inhomogeneous temperature distribution within the refractory components or linings.

If these stresses exceed the strength of the refractory material, a crack will form. Even if, in the case of thermal spalling, cracks can be initiated in the infiltrated layer of the refractory lining, they also spread to the non-infiltrated area, resulting in an unspecific loss of material (i.e. both infiltrated and non-infiltrated material).
Structural spalling, which is more rarely also referred to as chemical spalling, is a direct consequence of a material change at the face of a refractory lining exposed to a process medium able to infiltrate into it. The infiltration of a refractory material by process media does not necessarily lead directly to material loss, at least as long as the matrix of the refractory material is not significantly chemically dissolved by the process medium. In this case, the matrix components may either display a degree of inertness towards the process medium, or they may react with it. While in the former case, the overall chemical composition in the infiltrated zone is altered as well, the physical changes in the matrix prevail. The open porosity is filled by the process medium, which primarily leads to a reduction in porosity as well as an alteration of the thermal conductivity. However, as soon as new mineral phases form, which typically have a lower density and therefore expand into the ceramic structure as they form, local stresses occur. This induces the formation of cracks in the infiltrated layer of the refractory material and at the transition zone to the non-infiltrated material. With time, these cracks coalesce and grow. Eventually, the cracks reach a critical length and a fracture occurs. Large flacks of infiltrated material peel out parallel to the hot side of the refractory lining (discontinuous wear).

INVESTIGATION OF THE STRUCTURAL SPALLING
Damage to refractory linings as a result of structural spalling can be observed in almost all high-temperature industrial vessels and furnaces. Nevertheless, and despite its importance, publications on this phenomenon are sparse and fragmented. Remarkable reports on this phenomenon are yet known for steel ladles [4], tapping gas generators [5], electric arc furnaces [6], Ruhrstahl-Heraeus (RH) degassers [7], copper converters [8] and cement rotary kilns [9]. However, all these contributions are post-mortem examinations of excavated materials from decommissioned refractory linings of industrial vessels and furnace. In most cases, the presence of macrocracks in the vicinity of the transition zone to the non-infiltrated material and the resulting progressive spalling of the infiltrated layer is clearly visible. In particular, the infiltration by process media and the formation of new phases was demonstrated in the aforementioned studies using SEM examinations with spatially resolved microanalysis (EDX). Besides this, the number of specific studies in which the phenomenon of structural spalling was reproduced and investigated in the laboratory under controlled conditions is extremely limited [10-11]. This means that there is a lack of knowledge that could lead to unequivocal conclusions on how to improve the material’s behaviour. Instead, attempts made to improve the resistance of refractory materials to structural spalling are typically either based on the evaluation of individual cases (post-mortem studies) [5-7,9]. Or they rely on minimising the infiltration susceptibility of refractory materials, thereby ideally preventing structural spalling before it occurs, in combination with an optimisation of the resistance to thermal shocks [12]. In such cases, the resistance to infiltration by a process medium and resistance to

thermal spalling/shocks are usually investigated independently of each other. To that end, it is common practice to use standardized testing procedures. However, while these are rather efficient to compare the performance of the refractory products under the conditions defined in the said standards, their practical relevance is questionable, since these enforce testing conditions that typically do not align with the service conditions of refractory products. Finally, and especially if these technological properties (resistance to infiltration by a process medium and resistance to thermal shocks) cannot be improved concomitantly, or at different levels, it is completely unclear which property should be prioritised in order to improve the resistance to structural spalling.
In the light of all this, a new testing strategy has been elaborated to investigate the resistance to structural spalling in application-oriented manner.

MATERIALS AND METHODES

Testing strategy

To mimic the process of structural spalling on a laboratory scale, a two steps procedure was implemented:

1. *Preparation of infiltrated test pieces*: a model refractory castable was infiltrated in a controlled manner using modified cup test. Then, cylindrical test pieces (50 x 50 mm) were prepared out of the infiltrated model refractory castables.
2. *Thermal cycling*: the partially infiltrated test pieces were exposed to high temperature thermal shocks to simulate operational thermal cycling of refractory material used as wear lining in the steel making industry, more especially the filling and emptying of metallurgical vessels for the steel production. The structural spalling process itself, or more generally the progressive damaging of the test pieces, was assessed in-situ and contactless with laser-ultrasonic measurements.

Composition of model refractory castables and preparation

A model self-flowing calcium aluminate bonded high alumina refractory castable was selected for the present investigation (Tab. 1). The main aggregates are tabular alumina T60/T64 (Almatis, Ludwigshafen, Germany), a sintered α-alumina material (Al_2O_3 > 99 wt.%) that has been fully densified by rapid sintering at temperatures in excess of 1800°C, reactive alumina (CTC 20 and RG 4000, Almatis, Ludwigshafen, Germany), very fine alumina particles with excellent sintering activity and, as binder, Secar 712 (Imerys S.A., Paris, France), a cement composed purely of calcium aluminate phases CA and CA_2 with improved time stability. The polycarboxylate ether dispersing agent Castament FS 60 (BASF SE, Ludwigshafen, Germany) was used to disperse the model refractory castable (MRC).
After mixing in an intensive mixer (type R05, Maschinenfabrik Gustav Eirich) the model refractory castables were cast into custom-made moulds to produce special crucibles for the preparation of the partially infiltrated 50 x 50 mm cylindrical test pieces. All cast crucibles were stored in a climatic chamber for 48 h at 20 °C and 95 % relative humidity to cure. Then they were demoulded to be dried at 100 °C for 24 h and finally pre-fired at 800 °C for 2 h.

Tab. 1: Composition of the model high alumina refractory castables.

Castable (MRC)	wt%
Tabular alumina T60/T64	
3,0 - 6.0 mm	16
1,0 - 3.0 mm	21
0,5 - 1 mm	11
0,2 – 0,6 mm	10
0 - 0,2 mm	11
0 – 0,045 mm	9
Reactive alumina	
CTC 20	10
RG 4000	7
CA cement (Secar 712)	5
Dispersing agent (Castament FS 60)	0,15
Water	4,7

Controlled infiltration of the test pieces

Infiltrated test pieces were prepared using a modified corrosion cup test setup. As mentioned above, special crucibles were produced by casting the model refractory castable into 3D-printed moulds. Rather than being simple cuboids with a cylindrical hollow space inside, the crucibles' hollow space is partially filled with a 50 mm diameter cylinder. This leaves a constant gap between the cylinder and the inner surface of the rest of the crucible, as well as a hollow cylindrical space above the cylinder (Fig. 1, first step). This free space is then filled with a mix of compounds (Tab. 2) to form a slag at high temperatures (Fig. 1, second step). The filled crucible is then fired at 1500 °C for two hours (Fig. 1, third step). Finally, the inner cylinder is drilled free from the crucible and cut to a height of 50 mm. The result is a 50 x 50 mm cylindrical test piece with a partially infiltrated lateral face (Fig. 1, fourth step).
The depth of the infiltration is largely proportional to the width of the gap left between the cylinder inside the crucible and the inner surface of the rest of the crucible. By using different inserts in the 3D-printed mould, the width of gap can be varied and therefore the depth of the infiltration adjusted. In the present study only one gap width was used and therefore all infiltrated test pieces show a very similar infiltration depth, namely circa 4 mm.

Tab. 2: Mix of compounds that form a slag at high temperature.

Compound	wt%
$CaCO_3$	50,2
SiO_2	13,5
Fe_2O_3	22,4
Mn_2O_3	4,5
$MgCO_3$	9,4
Sum	100

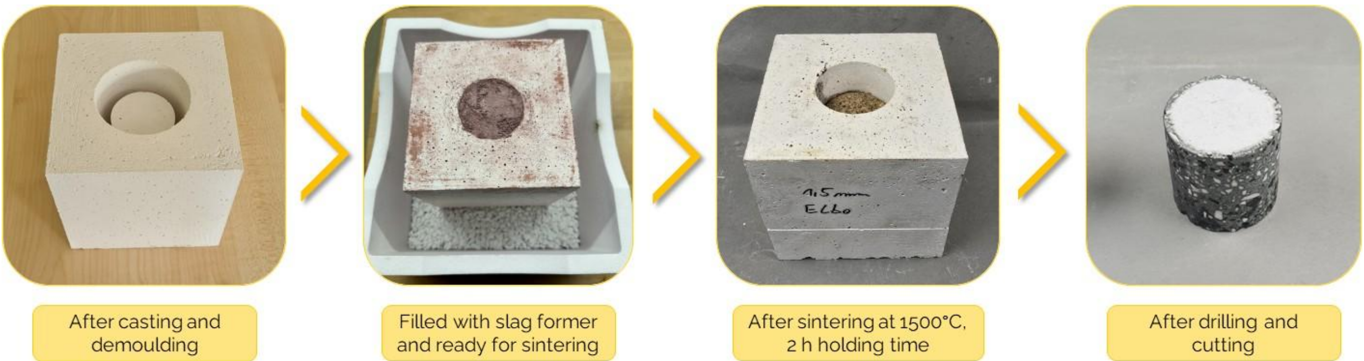

Fig. 1: Step-by-step preparation of the infiltrated test pieces.

High temperature thermal shocks

One crucial challenge was to perform efficient thermal cycling at high temperature. To achieve this, the partially infiltrated test piece is conveyed between two chambers in a new testing system (Fig. 2). The bottom chamber serves as a standby furnace with the ability to heat or cool the test piece to a predetermined temperature (Fig. 2 (b)). Ascending thermal shocks are achieved in the upper chamber by transporting the test piece into a carbon ring which is inductively heated to incandescence (chamber 1). The intensive radiation emitted by the carbon ring (susceptor) is particularly efficient to raise the surface temperature of the test piece inside the carbon ring quickly over 1800 °C (Fig. 2 (a)). A lifting device ensures the transport of the test piece (placed on an alumina tube) through the vertically stacked chambers. The system is continuously flushed with inert gas to protect the carbon ring in the chamber 1.

During the thermal cycling, stresses of sufficient magnitude to damage the test piece are generated. The impact of the thermal shocks is assessed quantitatively after each thermal shock in the chamber 1 at 800 °C using a laser-ultrasonic system applying an ultrasonic pulse velocity test [14]. The change of the ultrasonic velocity inside the test piece reflects the microstructural evolution of the refractory material. Especially, its decrease usually indicates the deterioration of the mechanical properties of the test pieces exposed to thermal shocks, typically as the result of crack formation. For a better insight, the level of damage is quantified using the dimensionless damage parameter D according to Kachanov [13]:

$$D = 1 - \left(\frac{v}{v_0}\right)^2 \qquad (1)$$

where v is the ultrasonic velocity as it propagates through the test piece after thermal shocking and v_0 is the initial ultrasonic velocity as it propagates through the test piece before exposure to thermal shocks. Therefore, D = 0 means no damage, while an increase in the D value signifies increasing damage.

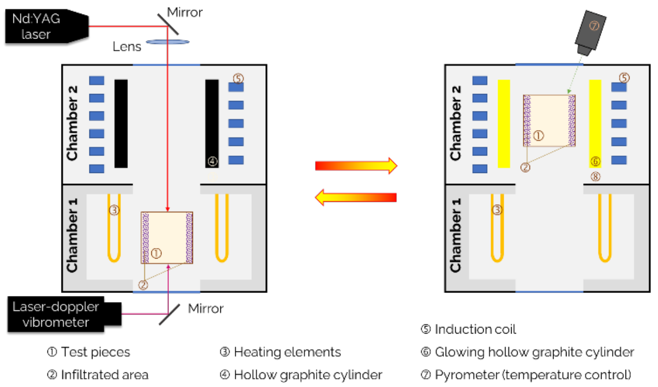

*Fig. 2: Schematic visualization of the thermal shock testing system and the testing procedure: **(on the left)** Preheating and tempering in the chamber 1, **(on the right)** ascending thermal shock through driving the test piece into an inductively heated carbon ring in the chamber 2.*

With an emphasis on being relevant for an application in the steel making industry, following testing conditions were selected:

- Lower temperature (chamber 2): 800 °C
- Higher temperature (chamber 1): 1600 °C

Five ascending thermal shock cycles were applied to the investigated test pieces as described above. A dwell time of 30 min in the bottom chamber (chamber 2) was implemented to ensure the temperature homogeneity of the test pieces. A shorter dwell time (15 min) was used in the upper chamber (chamber 1). Thermal stresses tend to quickly reach a maximum during thermal shocking, which roughly corresponds to the maximum temperature difference inside the test piece, namely before its core starts to heat up and the thermal gradient inside of the test pieces gradually flattens out. Accordingly, there is no need to reach temperature homogeneity after applying a thermal shock. The testing conditions implemented aimed to mimic the filling and emptying of a steel ladle. When filled with liquid steel, the refractory wear lining experiences temperatures above 1600 °C and ideally should not drop too low when emptied, in order to avoid significant heat loss.

RESULTS AND DISCUSSIONS

As expected, the damaging of the test pieces increased with an increasing number of thermal shocks. However, it seems that most of the assessed damage occurs during the first thermal shocks, with a subsequent reduction in the damaging rate (Fig. 3 and Tab. 3). It is also noteworthy that very similar results are obtained for repeated measurements using the same type of test pieces, namely either the non-infiltrated or the infiltrated ones. With the necessary cautiousness regarding the very limited number of test pieces involved in the present study, this tends to indicate a quite satisfactory repeatability of the measurements.

Regarding the non-infiltrated test pieces (namely pure thermal spalling) a rather gradual damaging is observed, which only slowed down after the 4th thermal shocks and reaching a value D of 0,4 after 5 thermal shocks. In contrast, infiltrated test pieces sustained already after the first thermal shock massive damaging (D > 0,6), followed by a slowing progression of the damage to reach a value of almost 0,9 after 5 thermal shocks. The partial infiltration of the material by the process media strongly impacted the response of the test pieces to the thermal shocks. This clearly highlighted the detrimental coupling effect between the infiltration/reaction with process media and the thermal shocks applied to the refractory materials, leading ultimately to structural spalling.

Tab. 3: Summary of the values for the damage parameter D after a given number of thermal shocks for the investigated test pieces. Each value of D is based on three laser ultrasonic measurements.

Number of thermal shocks	**Damage parameter D / -**				
	Non-infiltrated - 1	Non-infiltrated - 2	infiltrated - 1	infiltrated - 2	infiltrated - 3
0	0,00	0,00	0,00	0,00	0,00
1	0,03 ± 0,02	0,12 ± 0,05	0,61 ± 0,03	0,67 ± 0,11	0,71 ± 0,08
2	0,20 ± 0,03	0,21 ± 0,07	0,86 ± 0,06	0,71 ± 0,07	0,81 ± 0,09
3	0,26 ± 0,04	0,34 ± 0,04		0,83 ± 0,01	0,84 ± 0,01
4	0,38 ± 0,02	0,44 ± 0,02	0,89 ± 0,02	0,85 ± 0,01	0,86 ± 0,01
5	0,42 ± 0,03	0,41 ± 0,03	0,88 ± 0,06	0,87 ± 0,01	0,89 ± 0,01

Visual inspection of the test pieces after exposure to thermal shocks makes the extent of the damage even clearer. Macrocracks could be observed at the surface of all investigated test pieces and more distinctly still in the cross-sections after cutting the test pieces in half (Fig. 4). However, while non-infiltrated test pieces tend to display rather few sharp macrocracks, partially infiltrated test pieces present typically a denser network of larger macrocracks (Fig. 4 (a). In both cases, cracks that run in the middle of the test pieces are assumed to be those that, in practice, would lead to thermal spalling. Additionally, in partially infiltrated test pieces, macrocracks running in the infiltrated area, or in the transition zone to the non-infiltrated area, and widely parallel to the surface can be systematically observed (Fig. 4 (b)). The changes in composition and mineralogy induced by the infiltration and reactions between the process medium (slag) and the refractory material led to a significant alteration of the properties of the infiltrated area. On the one hand, this seems to amplify the thermal stresses resulting from the thermal shocks, and accordingly intensifying the overall damaging in the refractory material (thermal spalling). On the other hand, this apparently weakens the infiltrated area and transition zone to the non-infiltrated area of the refractory material, and/or gives rise to local stresses, leading to the formation and propagation of cracks in these areas, and ultimately the flaking of the infiltrated part of the refractory material (structural spalling).

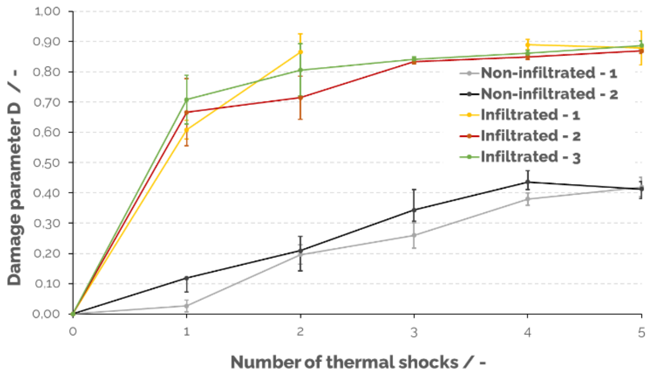

Fig. 3: Evolution of the damage parameter D in function of the number of thermal shocks experienced by the test pieces (based on measurements performed at 800 °C after each thermal shock).

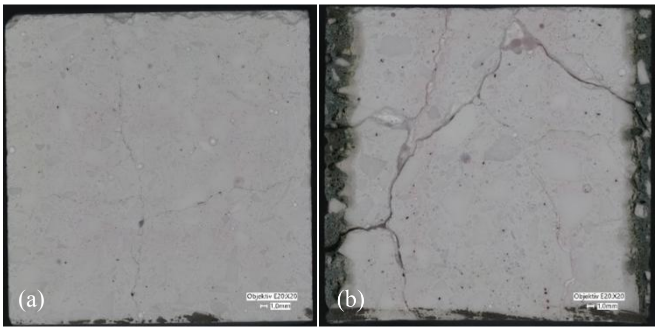

*Fig. 4: Digital microscope image of test pieces' cross-sections after exposure to thermal shocks **(a)** non-infiltrated test piece, **(b)** partially infiltrated test piece.*

CONCLUSIONS

In service refractory products, as lining of industrial vessels and furnaces enabling high temperature processes, get infiltrated by the process media (liquid metal, slag or gases), hence altering locally their thermomechanical properties. This promotes the formation of cracks or even the spalling of the infiltrated areas (structural spalling) during operational thermal cycling.

In order to directly investigate the resistance to thermal spalling of refractory materials, a new application-oriented testing strategy, able to simulate and assess the impact of practice-relevant thermal shocks on the degradation of partly infiltrated refractory materials used as wear lining in the metallurgical industry has been developed. Test pieces made of refractory castables were infiltrated in a controlled manner and then exposed to high temperature thermal shocks while the evolution of their elastic properties was assessed in-situ and contactless after each thermal shock using laser-ultrasonic measurements. The intensity and temperature range in which the thermal shocks are performed can be adjusted to simulate other processes involving refractory linings, or even change of the operating conditions for an established process.

With each thermal shock applied to the test pieces, damage accumulated into the refractory material. The first thermal shocks induced the higher share of damage, especially in partially infiltrated test pieces. These presented significantly more pronounced deterioration, both in quantitative assessments during the thermal shocks cycling (laser-ultrasonic measurements) and visual observations after the cooling the test pieces back to room temperature (macrocracks), than the thermo-shocked non-infiltrated test pieces. Furthermore, cracks running widely parallel to the surface were clearly visible a in the infiltrated area, or in the transition zone to the non-infiltrated area. The infiltration of process media not only induced structural spalling, but intensified the thermal spalling.

The developed testing procedure has been proven efficient and reliable to investigate the structural spalling of refractory materials. However, it is still to clarify, what is the best strategy to increase the resistance to thermal shocks for partially infiltrated refractory materials when both the resistance to infiltration and to thermal spalling cannot be improved simultaneously or to different levels.

ACKNOWLEDGEMENTS

This project has been supported by the Federal Ministry for Economic Affairs and Energy (BMWE) on the basis of a decision by the German Bundestag.

REFERENCES

[1] Cannio, M., Boccaccini, D.N., Romagnoli, M. New Methods for the Assessment of Thermal Shock Resistance in Refractory Materials. In: Hetnarski, R.B. (eds) Encyclopedia of Thermal Stresses. Springer, Dordrecht. 2015

[2] Mocciaro, A., Anaya, R., Hernández, M. F., Richard, D., & Rendtorff, N. M. Experimental and Theoretical Study of the Thermal Shock Behavior of Insulating Refractory Materials. Ceramics, 8(1), 2025

[3] Poirier, J., Rigaud, M. Corrosion of Refractories: The Fundamentals, in: F.I.R.E Compendium Series, Baden-Baden, Göller Verllag GmbH, 2017

[4] Matsui, T., Taki, N. Refractory Technology of Ladle, Nippon Steel Technical Report, 2020, p. 51-54

[5] Bennett, J.P., Petty, A.V., Kwon, K.-S., Thomas, H., Krabbe, R. Chemical corrosion of refractory liners in air-cooled slagging gasifiers by slag from carbon feedstock, in: Proceeding of the Unified International Technical Conference on Refractories (UNITECR), 2007, p. 444–447

[6] Boymanns, G., Dreimann, S., Corrosion of refractory materials in a direct arc furnace for melting ashes from grate firing and fly, in: Proceedings of the 48th International Conference on Refractories, Aachen, Germany, 2005, p. 118–120

[7] Asano, K., Ootuki, Y., Goto, K., Shikano, H., Yamamoto, H., Tamaki, K. Corrosion of fired magnesia chromite bricks BY CaO-CaF_2 slags and development of highly durable magnesia chromite brick, in: Proceedings of the 31st International Conference on Refractories, Aachen, 1988, p. 317-327

[8] Goni, C., Barbés, M. F., Bazán, V., Brandaleze, E. The mechanism of thermal spalling in the wear of the Pierce-Smith copper converter, Journal of the Ceramic Society of Japan, p. 672–675

[9] Prestes, E., Chinelatto, A. S. A., Resende, W. S. Post mortem analysis of burned magnesia-chromite brick used in short rotary furnace of secondary lead smelting, Cerâmica, 55, 2009, p. 61–66

[10] Imai, K., Takada, T., Development of Chamotte Brick Preventing Structural Spalling for Calcining Zone of Cement Rotary Kiln. Taikabutsu overseas, 29(3), 2009, p.219 - 223

[11] Loison, L., Sassi, M., Tonnesen, T., de Bilbao, E., Telle, R., Poirier J. Differences in the Corrosive Spalling Behavior of Alumina-Rich Castables: Microstructural and Crystallographic Considerations of Alumina and Calcium Aluminate Matrices. Ceramics 3, 2020, p. 223-234

[12] Kakihara, M., Suto, M., Tad, H., Improvement of Spalling Resistance on Low Carbon MgO-C Bricks, in: Proceeding of the Unified International Technical Conference on Refractories (UNITECR), 2011.

[13] Kachanov L.M.: Introduction to Continuum Damage Mechanics. Mechanics of Elastic Stability. Dordrecht, Boston, Lancaster: Martinus Nijhoff Publishers, 1986

[14] Brochen, E., Dannert, C., Esch, S., Kohns, P., Ankerhold, G. Application of the laser ultrasonic technology to the characterisation of refractory materials, In: Proceedings of the 65th International Conference on Refractories, Aachen, 2022.